

AUKT: Adaptive Uncertainty-Guided Knowledge Transfer with Conformal Prediction

Rui Liu¹ Peng Gao² Yu Shen³ Ming Lin¹ Pratap Tokekare¹

Abstract

Knowledge transfer between teacher and student models has proven effective across various machine learning applications. However, challenges arise when the teacher's predictions are noisy, or the data domain during student training shifts from the teacher's pretraining data. In such scenarios, blindly relying on the teacher's predictions can lead to suboptimal knowledge transfer. To address these challenges, we propose a novel and universal framework, Adaptive Uncertainty-guided Knowledge Transfer (AUKT), which leverages Conformal Prediction (CP) to dynamically adjust the student's reliance on the teacher's guidance based on the teacher's prediction uncertainty. CP is a distribution-free, model-agnostic approach that provides reliable prediction sets with statistical coverage guarantees and minimal computational overhead. This adaptive mechanism mitigates the risk of learning undesirable or incorrect knowledge. We validate the proposed framework across diverse applications, including image classification, imitation-guided reinforcement learning, and autonomous driving. Experimental results consistently demonstrate that our approach improves performance, robustness and transferability, offering a promising direction for enhanced knowledge transfer in real-world applications.

1. Introduction

In many machine learning applications, knowledge transfer (Hinton, 2015; Romero et al., 2014; Zagoruyko & Komodakis, 2016; Passalis & Tefas, 2018; Kim et al., 2018; Wang et al., 2023; Xue et al., 2022; Huo et al., 2024; Gu et al., 2023; Jin et al., 2023; Sun et al., 2024) from teacher models to student models is a valuable strategy that allows improved performance and practical deployment in real-

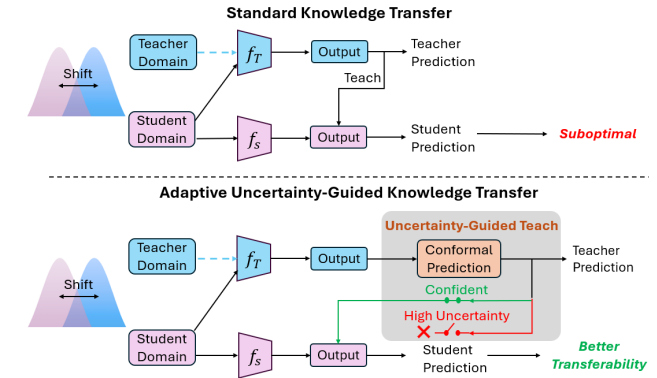


Figure 1. Comparison of standard knowledge transfer and AUKT. f_T and f_S denote the teacher and student models, with f_T pretrained on the teacher domain. The top panel shows standard knowledge transfer, where the student strictly follows the teacher, often leading to suboptimal performance under domain shifts. The bottom panel illustrates AUKT, which leverages conformal prediction to adjust teacher guidance based on prediction uncertainty, balancing teacher knowledge exploitation with student exploration for improved transferability.

world scenarios. The teacher models, composed of larger networks or access to multi-modalities, often exhibit superior performance but come with significant computational costs, making them unsuitable for resource-constrained environments. In contrast, student models are more lightweight (Gu et al., 2023) or designed to work with reduced data modalities (Shen et al., 2023) during testing, making them practical for real-world applications. The teacher-student framework allows the teacher models to provide predictions or insights that guide the student models' learning process. This can involve transferring knowledge from a larger network to a smaller one (Hinton, 2015; Romero et al., 2014; Zagoruyko & Komodakis, 2016), adapting multimodal teacher models to unimodal student models (Shen et al., 2023; Wang et al., 2023; Xue et al., 2022; Huo et al., 2024), or using pretrained imitation learning (IL) policies to bootstrap reinforcement learning (RL) agents (Hu et al., 2023; Bhaskar et al., 2024).

Traditional teacher-student frameworks often assume that the teacher's predictions are always reliable, using them as guidance for the student's learning. However, a key challenge arises when domain shifts occur between the data used

¹University of Maryland, College Park ²North Carolina State University ³Adobe Research. Correspondence to: Rui Liu <rui.liu@umd.edu>.

for pretraining the teacher and the data available for training the student. For instance, in transferring knowledge from large language models (LLMs) to student models for downstream tasks (Yang et al., 2024; Saad-Falcon et al., 2023), the student’s domain data may differ significantly from the pretraining data of the LLMs. Addressing this disparity typically requires retraining or fine-tuning the teacher model on the student’s domain (Yang et al., 2024; Saad-Falcon et al., 2023), but this process might be computationally expensive or impractical. For pretrained teacher models, domain shifts can introduce error in the teachers’ predictions, undermining their reliability. Blindly relying on the teacher in these scenarios will lead to suboptimal knowledge transfer, as the student may overfit to incorrect or uncertain guidance. This over-reliance restricts the student’s ability to explore independently and adapt effectively to new or noisy environments. These limitations are especially problematic in real-world applications, where dynamic and uncertain conditions are commonplace. Addressing such issues is crucial for improving the performance and transferability of knowledge transfer systems.

Conformal prediction (CP) (Angelopoulos et al., 2020; Angelopoulos & Bates, 2021; Mossina et al., 2024; Karimi & Samavi, 2023; Tibshirani et al., 2019; Shafer & Vovk, 2008; Vovk et al., 2020) is a non-parametric, distribution-free, and model-agnostic framework that provides reliable prediction sets with statistical coverage guarantees, enabling robust decision-making under data or model uncertainty. Leveraging CP, we propose a novel framework, Adaptive Uncertainty-Guided Knowledge Transfer (**AUKT**), to address key challenges in knowledge transfer systems. We show a comparison between conventional knowledge transfer methods and **AUKT** in Fig. 1. **AUKT** quantifies the teacher’s prediction uncertainty and uses it to dynamically determine the extent to which the student should rely on the teacher’s guidance. Specifically, when the teacher exhibits high confidence in its predictions, the student prioritizes the teacher’s guidance. Conversely, when the confidence is low, the student reduces its reliance on the teacher and explores the data more independently, potentially discovering new patterns or adapting better to noisy or domain-shifted data. **AUKT** is a general framework applicable to diverse teacher-student architectures, including model compression (larger to smaller networks), modality reduction (multimodal to unimodal networks), and imitation-to-reinforcement learning (pretrained policies to RL agents). We validate **AUKT** across diverse tasks, including image classification, imitation-guided reinforcement learning, and autonomous driving.

Here, we ask the question: *Can we improve the student model’s performance beyond standard knowledge transfer methods when there are domain shifts between the teacher’s pretraining data and the student’s training data, or when*

the teacher’s predictions are noisy? Additionally, there can be cases of teacher underperformance where the pre-trained teacher model performs worse than the student model trained from scratch on the student domain data, likely due to significant domain shifts. In such cases, we investigate: *Can the teacher model still provide useful knowledge to improve the student model’s performance beyond what is achievable when training from scratch?* This investigation especially differentiates **AUKT** from previous knowledge transfer methods, which often assume that the teacher’s performance exceeds that of the student model.

Unlike traditional teacher-student frameworks, our approach offers several unique advantages. We summarize the key contributions of our work as follows:

- We propose **AUKT**, a novel framework that leverages conformal prediction to efficiently quantify the uncertainty in the teacher’s predictions for knowledge transfer systems. By adaptively adjusting the teacher’s influence based on its confidence, **AUKT** ensures effective student learning without over-relying on unreliable guidance, particularly in domain-shifted scenarios.
- **AUKT** demonstrates the ability to still leverage useful “dark knowledge” from the teacher model to improve student performance, even when the teacher is underperforming due to significant domain shifts. This is a notable distinction from conventional knowledge transfer methods, which assume that the teacher always performs better than the student.
- **AUKT** is universal and domain-agnostic, making it applicable to diverse tasks. We validate **AUKT** across a range of applications, including image classification, imitation-guided reinforcement learning and autonomous driving, demonstrating improvements in performance, as well as enhanced robustness and transferability compared to conventional knowledge transfer methods.

2. Related Work

2.1. Knowledge Transfer

Knowledge transfer methods aim to adapt information from one network, modality, or learning paradigm to another. For instance, Hinton (2015); Jin et al. (2023); Sun et al. (2024) focused on transferring soft probabilities from the teachers’ logits to guide student models, whereas Romero et al. (2014); Zagoruyko & Komodakis (2016); Passalis & Tefas (2018); Kim et al. (2018) emphasized transferring intermediate features from the teacher to the student. These approaches primarily address knowledge transfer from larger teacher networks to smaller student networks. Cross-modality transfer has also been extensively explored. Wang et al. (2023) introduced a prototype-based distillation method to handle missing modalities in medical image segmentation, where a multi-modality teacher guides a

single-modality student. Similarly, Feng et al. (2023) distilled knowledge from an RGB-Thermal teacher model to a Thermal-only student model for semantic scene understanding. Shen et al. (2023) proposed Auxiliary Modality Learning (AML), where a teacher model with access to multiple modalities transfers knowledge to a student model that operates on reduced modalities during testing. Additionally, knowledge transfer across different learning paradigms has been investigated, such as in (Hu et al., 2023; Bhaskar et al., 2024), where pretrained imitation learning (IL) policies were used to guide reinforcement learning (RL) agents.

A limitation of most existing knowledge transfer frameworks is their reliance on static guidance, which assumes the teacher’s predictions are consistently reliable and always superior to the student’s. This assumption often fails under significant domain shifts, where the teacher’s predictions may become unreliable, ultimately hindering the student’s learning. In contrast, **AUKT** introduces a principled approach to uncertainty-aware guidance that adaptively adjusts the teacher’s influence based on its prediction uncertainty, ensuring that the student learns effectively without over-relying on potentially misleading guidance.

2.2. Uncertainty-Aware Learning

Quantifying uncertainty (Abdar et al., 2021; Kwon et al., 2020; Karimi & Samavi, 2023) in machine learning systems has become a critical aspect, especially in safety-critical domains. For example, Edupuganti et al. (2020) quantified uncertainty in MRI reconstruction with deep learning models, while Kwon et al. (2020) employed Bayesian neural networks for uncertainty estimation in medical image classification. Similarly, Michelmore et al. (2020) evaluated uncertainty in end-to-end Bayesian controllers for autonomous driving, (Gao et al., 2023; Gao & Zhang, 2021) leverage uncertainty quantification in human-robot interaction, and Zhao et al. (2024) utilized Monte Carlo dropout for real-time uncertainty quantification in object detection for autonomous vehicles.

Despite the progress in uncertainty-aware learning, most prior works focus on quantifying uncertainty in standalone models, with less exploration of its integration into teacher-student knowledge transfer frameworks. In this context, uncertainty remains underexplored as a mechanism to modulate the interaction between teacher and student models dynamically. To bridge this gap, our approach leverages conformal prediction as a principled mechanism for uncertainty quantification. By integrating uncertainty awareness into the learning process, our method adaptively adjusts the teacher’s guidance, enabling the student to learn effectively while reducing the risk of overfitting to unreliable teacher predictions.

2.3. Conformal Prediction

Conformal prediction (CP) (Angelopoulos et al., 2020; Angelopoulos & Bates, 2021; Shafer & Vovk, 2008) is a nonparametric, distribution-free, and model-agnostic framework designed to provide reliable prediction sets with statistical coverage guarantees. In machine learning systems, CP has primarily been utilized for post-hoc uncertainty calibration due to its computational efficiency. For instance, Angelopoulos et al. (2020) introduced an algorithm that adapts any image classifier to output predictive sets containing the true label with a user-specified probability. Mossina et al. (2024) proposed a computationally lightweight approach to quantify predictive uncertainty in semantic image segmentation using CP. Similarly, Lu et al. (2022) applied CP to deep learning models for grading the severity of spinal stenosis in lumbar spine MRI, while Karimi & Samavi (2023) leveraged CP to measure uncertainty in deep learning models.

Despite these advancements, the application of CP in dynamic decision-making frameworks, such as adaptive knowledge transfer, remains underexplored. In this work, we extend CP to the domain of knowledge transfer, utilizing it as a foundation for adaptive, uncertainty-guided learning. By quantifying the teacher model’s prediction uncertainty, we enable the student model to dynamically adjust its reliance on the teacher, effectively balancing the integration of pretrained knowledge with independent exploration.

3. Approach

3.1. Preliminaries

In our framework, we leverage Conformal Prediction (CP) to quantify the teacher’s prediction uncertainty and guide knowledge transfer. CP is a distribution-free method that provides prediction sets or intervals with guaranteed coverage levels, independent of the underlying model (Angelopoulos & Bates, 2021; Shafer & Vovk, 2008).

CP uses a nonconformity score s to measure how unusual a prediction is for a new test input, based on a calibration set, a held-out dataset used to compute the empirical distribution of nonconformity scores. The score s can be defined in various ways, such as residuals (e.g., $|\bar{y} - \hat{y}(\bar{x})|$ for regression) or confidence scores (e.g., $1 - p_{\hat{y}}(\bar{x})$ for classification), where \bar{y} is the ground truth and $\hat{y}(\bar{x})$ is the model’s prediction for an input \bar{x} in the calibration set. Additional examples can be found in (Angelopoulos & Bates, 2021; Shafer & Vovk, 2008). From the calibration set, the $(1 - \alpha)$ quantile $q_{1-\alpha}$ of the nonconformity scores is computed, representing the threshold below which $1 - \alpha$ of the data falls, where α is the allowable error rate. A prediction set for a test input x_{test} includes all labels y satisfying $s(x_{\text{test}}, y) \leq q_{1-\alpha}$, ensuring a coverage probability of $1 - \alpha$, assuming the calibration and test data are from the same distribution (Angelopoulos & Bates, 2021).

3.2. Problem Definition

We consider a knowledge transfer problem where a student model learns from a teacher model. Conventional knowledge transfer methods often assume consistently superior teacher performance. However, knowledge transfer becomes challenging when domain shifts occur, leading to uncertainty in the teacher model’s prediction and suboptimal knowledge transfer.

To address these challenges, we propose an Adaptive Uncertainty-Guided Knowledge Transfer (**AUKT**) framework to improve the robustness and transferability of knowledge transfer systems. Formally, let the teacher domain data be denoted as \mathcal{D}_T with distribution P_T , and the student domain data as \mathcal{D}_S with distribution P_S . We represent the teacher model pretrained on \mathcal{D}_T as $f_T : \mathcal{X} \rightarrow \mathcal{Y}$, and the student model as $f_S : \mathcal{X} \rightarrow \mathcal{Y}$, where \mathcal{X} is the input space and \mathcal{Y} is the output space. In this framework, we do not retrain or finetune the teacher model f_T on the student domain \mathcal{D}_S , as this can be computationally prohibitive. Instead, we aim to transfer the knowledge from f_T to f_S , with the goal of improving the performance of f_S on \mathcal{D}_S compared to conventional knowledge transfer approaches or training the student model from scratch. This is particularly important when \mathcal{D}_S differs from \mathcal{D}_T (i.e., $P_S \neq P_T$), making $f_T(x)$ uncertain for input $x \in \mathcal{D}_S$.

3.3. Adaptive Uncertainty-Guided Knowledge Transfer

Our approach aims to improve knowledge transfer by leveraging the prediction uncertainty of the teacher model to guide the student’s learning process, especially in the presence of domain shifts. Given a student domain \mathcal{D}_S , we split it into three subsets: the student training set $\mathcal{D}_{\text{train}}^S$, used to train the student model f_S ; the calibration set \mathcal{D}_{cal} , used to transform any heuristic measure of uncertainty from the pretrained teacher model f_T into a rigorous one; and the testing set $\mathcal{D}_{\text{test}}$ for validate the model performance. The student training set $\mathcal{D}_{\text{train}}^S$ also serves as the testing set for f_T in CP-based uncertainty quantification. This is because in the knowledge transfer process, both the teacher and student models take the same input data, with the student learning from the teacher’s predictions. We assume that $\mathcal{D}_{\text{train}}^S$ and \mathcal{D}_{cal} come from the same distribution, satisfying the assumption of CP. **AUKT** is a general framework, we show how to use it in both supervised and imitation-guided reinforcement learning settings with minimal changes.

3.3.1. SUPERVISED LEARNING

Given a pretrained teacher model f_T and the calibration set \mathcal{D}_{cal} , for each sample $(\bar{x}_i, \bar{y}_i) \in \mathcal{D}_{\text{cal}}$, we compute a nonconformity score s_i , where s_i can be residuals (e.g., $|\bar{y}_i - \hat{y}(\bar{x}_i)|$ for regression) or confidence scores (e.g., $1 - p_{\hat{y}}(\bar{x}_i)$ for classification), as described in Section 3.1, depending on the task. Using a predefined coverage level $1 - \alpha$, we compute the $(1 - \alpha)$ -quantile of these scores, denoted as

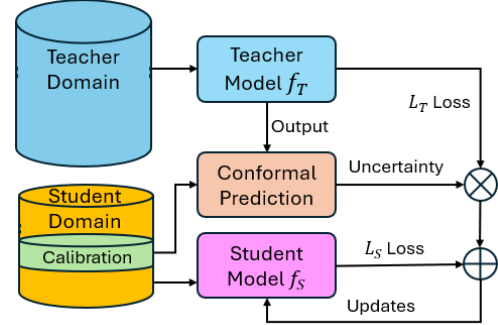


Figure 2. AUKT Approach Pipeline. The figure demonstrates our approach, **AUKT**, which dynamically adjusts the teacher’s guidance based on its prediction uncertainty using conformal prediction. This method balances the exploitation of teacher knowledge with student exploration itself, enabling better transferability of knowledge under domain shifts.

$q_{1-\alpha} = \text{Quantile}_{1-\alpha}(s_1, s_2, \dots, s_{|\mathcal{D}_{\text{cal}}|})$, which serves as a threshold for constructing prediction sets. For a test input x_{test} , we define the prediction set for the teacher model f_T as: $\mathcal{C}(x_{\text{test}}) = \{y \in \mathcal{Y} : s(x_{\text{test}}, y) \leq q_{1-\alpha}\}$, with the probability of the true label y_{test} falling within $\mathcal{C}(x_{\text{test}})$ satisfies $P(y_{\text{test}} \in \mathcal{C}(x_{\text{test}})) \geq 1 - \alpha$. To quantify uncertainty, we use the size of the prediction set $\mathcal{C}(x)$ for an input $x \in \mathcal{D}_{\text{train}}^S$. Specifically, we define the teacher model’s uncertainty as:

$$u_T(x) = g(|\mathcal{C}(x)|), \quad (1)$$

where g is a function that maps the size of the prediction set (e.g., the number of classes for classification or the interval length for regression) to an uncertainty value. Then we define the loss function of the adaptive uncertainty-guided knowledge transfer, which is

$$\mathcal{L} = \lambda_1 \mathcal{L}_S + w(x) \cdot \lambda_2 \mathcal{L}_T, \quad (2)$$

where \mathcal{L}_S is the student’s task loss (e.g., Cross Entropy loss), \mathcal{L}_T is the teacher guidance loss (e.g., KL divergence between student and teacher logits), λ_1 and λ_2 are the coefficients, and w is an uncertainty-based weight derived from the teacher model’s uncertainty u_T :

$$w(x) = h(u_T(x)), \quad (3)$$

where h is a function mapping uncertainty to the weight w . w approaches 1 when the teacher’s predictions are confident and decreases toward 0 as the uncertainty increases. We show the algorithm of **AUKT** in the Appendix A.1. We also provide a theoretical analysis to explain why **AUKT** outperforms standard knowledge transfer methods, please see the Appendix A.2.

Our approach dynamically adjusts the student’s reliance on the teacher based on prediction uncertainty. When the teacher is confident, the student follows its guidance, but as uncertainty rises, the student explores more independently. This balance between exploiting teacher knowledge and encouraging exploration helps the student avoid over-reliance

on uncertain predictions and generalize effectively, particularly in cases of domain shifts where the teacher’s pretrained knowledge may not transfer well. This ensures robust and reliable learning outcomes.

3.3.2. IMITATION-GUIDED REINFORCEMENT LEARNING

Consider a Markov Decision Process (MDP) defined by the tuple $\{\mathcal{S}, \mathcal{A}, \mathcal{P}, \mathcal{R}, \gamma\}$, where \mathcal{S} is the state space, \mathcal{A} is the action space, \mathcal{P} is the transition dynamics, \mathcal{R} is the reward function, and γ is the discount factor. We focus on off-policy RL methods due to their higher sample efficiency, leveraging past experiences and expert demonstrations.

To quantify uncertainty, we define a nonconformity score $s(s, a) = -\log \pi(a|s)$, measuring how “atypical” an action a is in state s for a policy π . Given a teacher model f_T (e.g., a pretrained imitation policy), we first collect calibration set $\mathcal{D}_{cal} = \{(s_i, a_i)\}_{i=1}^n$ by rolling out f_T in the student domain. For a predefined coverage level $1 - \alpha$, we compute the $(1 - \alpha)$ -quantile $q_{1-\alpha}$ of the nonconformity scores on \mathcal{D}_{cal} . For a test state s_{test} , we construct a conformal prediction set $\mathcal{C}(s_{test}) = \{a \in \mathcal{A} : s(s_{test}, a) \leq q_{1-\alpha}\}$, ensuring $P(a_{test} \in \mathcal{C}(s_{test})) \geq 1 - \alpha$. Unlike prior setups where only the teacher model is calibrated, here we calibrate both teacher model f_T and student model f_S . Since f_T is pretrained, its quantile $q_{1-\alpha}^T$ remains static, while the student’s quantile $q_{1-\alpha}^S$ is updating online during training. Using the corresponding prediction sets, the teacher and student uncertainties are defined as $u_T(s) = g(|\mathcal{C}_T(s)|)$ and $u_S(s) = g(|\mathcal{C}_S(s)|)$, respectively.

Similar to supervised learning, the total loss function is defined as: $\mathcal{L} = \mathcal{L}_S + w(s) \cdot \mathcal{L}_T$, where \mathcal{L}_S is the student’s task loss (e.g., $\mathbb{E}[-\log f_S(a|s) \cdot A(s, a)]$ with $A(s, a)$ as the advantage function), which corresponds to the RL objective. $\mathcal{L}_T = \mathbb{E}[\text{KL}(f_S(\cdot|s) \parallel f_T(\cdot|s))]$ is the KL divergence between the student’s policy and the teacher’s, serving as the teacher guidance loss. The weight w , defined as: $w(s) = h(u_T(s), u_S(s))$, is similar to Eq. 3 but incorporates the uncertainties of both teacher and student.

4. Experiments

To validate our approach, we conduct experiments across a diverse range of applications, including image classification, imitation-guided reinforcement learning, and autonomous driving.

4.1. Image Classification

In image classification, we evaluate the effectiveness of our framework in enhancing predictive performance compared to traditional knowledge transfer approaches. This evaluation is performed under different levels of domain shifts and noise. Specifically, we aim to address the two primary research questions: (1) Can we improve the performance of

the student model beyond standard knowledge transfer techniques? (2) When the teacher model is underperformance, can it still provide useful “dark knowledge” to enhance the performance of the student model beyond what is achievable by training from scratch?

Experimental Settings. We conduct our experiments on the CIFAR-100 dataset (Krizhevsky et al., 2009), which consists of 60K images, 50K for training and 10K for testing, across 100 distinct categories. In this section, we focus on knowledge transfer under two distinct settings: **Homogeneous Structure**, where both the teacher and student models share the same type of architecture (e.g., ResNet-32x4 and ResNet-8x4), and **Heterogeneous Structure**, where the teacher and student models are of different architectures (e.g., ResNet-32x4 and ShuffleNet-V1). We evaluate a wide range of neural network architectures, including ResNet (He et al., 2016), WRN (Zagoruyko, 2016), VGG (Simonyan, 2014), ShuffleNet-V1 (Zhang et al., 2018)/V2 (Ma et al., 2018), and MobileNet-V2 (Sandler et al., 2018). We introduce two levels of domain shifts. In Level 1, the domain shift is relatively mild with Gaussian noise of zero mean and a standard deviation of 0.03. In Level 2, the shift is more pronounced with noise standard deviation increased to 0.05, which may lead to underperformance of the teacher model, where its performance is worse than that of the student model trained from scratch on the student training set. For further details on these two levels of domain shifts, please refer to the Appendix A.3.1.

To quantify the uncertainty of the pretrained teacher model f_T using conformal prediction, we utilize the RAPS algorithm as described in (Angelopoulos et al., 2020) with an error rate of $\alpha = 0.1$. For more details on the RAPS algorithm, please refer to (Angelopoulos et al., 2020). Given an input image x , we obtain the prediction set $|\mathcal{C}(x)|$ where the teacher model provides a set of candidate predictions. The prediction uncertainty of f_T in Eq. 1 is then defined as $u_T(x) = \frac{|\mathcal{C}(x)| - 1}{K - 1}$ (Vovk et al., 2016), where K is the total number of classes, which is 100 for the CIFAR-100 dataset. From this uncertainty definition, u_T takes values between 0 and 1. If f_T is confident with its prediction with a single class, u_T will be 0. Conversely, if the prediction is uncertain and contains multiple classes in the prediction set, u_T is larger than 0. To incorporate this uncertainty into the knowledge transfer process, we define the uncertainty-based weight in Eq. 3 as $w = 1$ if $u_T = 0$, $w = 0$ if $u_T > 0$ (Vovk et al., 2016). This weight helps adjust the influence of the teacher’s prediction on the student model, ensuring that confident predictions are more heavily relied upon while uncertain predictions have less influence. We follow the same experimental settings as in previous work (Tian et al., 2019; Sun et al., 2024) for the coefficients λ_1 and λ_2 , as well as other training details. Please refer to the Appendix A.3.3 for more details.

Table 1. Top-1 accuracy (%) of various knowledge transfer methods with and without **AUKT** on CIFAR-100 under homogeneous structure and domain shift Level 1. We use Δ to show performance gain relative to conventional knowledge transfer methods without **AUKT**. We highlight in orange deltas greater than 0.15, indicating non-trivial enhancement following the protocol in (Sun et al., 2024).

	ResNet110	ResNet56	ResNet32 \times 4	VGG13	WRN-40-2	WRN-40-2
Teacher	68.09	65.80	73.01	70.65	69.38	69.38
	68.09	65.80	73.01	70.65	69.38	69.38
Student	ResNet20	ResNet20	ResNet8 \times 4	VGG8	WRN-40-1	WRN-16-2
	67.70	67.70	70.20	68.07	69.33	71.40
KD (Hinton, 2015)	67.85	67.58	70.27	69.34	69.42	70.80
KD + AUKT	68.33	67.65	70.87	69.38	70.47	71.79
Δ	0.46	0.07	0.60	0.04	1.05	0.89
FitNet (Romero et al., 2014)	67.81	67.48	70.38	67.68	69.47	71.07
FitNet + AUKT	68.22	67.82	71.22	68.00	69.51	71.32
Δ	0.41	0.34	0.84	0.32	0.04	0.25
PKT (Passalis & Tefas, 2018)	67.50	67.33	70.51	67.90	69.46	71.29
PKT + AUKT	67.89	67.64	71.11	68.08	70.03	71.56
Δ	0.39	0.31	0.60	0.18	0.57	0.27
FT (Kim et al., 2018)	67.37	67.25	70.09	67.90	69.64	71.23
FT + AUKT	67.97	67.37	70.73	68.07	70.00	71.84
Δ	0.60	0.12	0.64	0.17	0.36	0.61

Table 2. Top-1 accuracy (%) of various knowledge transfer methods with and without **AUKT** on CIFAR-100 under homogeneous structure and domain shift Level 2 where the teacher models are underperforming. We use Δ to show performance gain relative to conventional knowledge transfer methods without **AUKT**. We highlight in orange deltas greater than 0.15, indicating non-trivial enhancement following the protocol in (Sun et al., 2024).

	ResNet110	ResNet56	ResNet32 \times 4	VGG13	WRN-40-2	WRN-40-2
Teacher	58.78	56.23	62.61	61.47	58.76	58.76
	58.78	56.23	62.61	61.47	58.76	58.76
Student	ResNet20	ResNet20	ResNet8 \times 4	VGG8	WRN-40-1	WRN-16-2
	66.70	66.70	69.14	67.08	69.12	70.59
KD (Hinton, 2015)	65.96	65.56	68.06	66.51	68.80	69.06
KD + AUKT	67.47	67.39	68.92	67.31	69.73	70.82
Δ	1.51	1.83	0.86	0.80	0.93	1.76
FitNet (Romero et al., 2014)	66.60	66.20	68.97	66.59	69.03	70.15
FitNet + AUKT	67.13	66.98	69.41	67.21	69.31	71.26
Δ	0.53	0.78	0.44	0.62	0.28	0.11
PKT (Passalis & Tefas, 2018)	66.58	66.13	69.32	67.08	68.83	70.34
PKT + AUKT	67.58	66.68	69.66	67.27	69.28	70.65
Δ	0.20	0.55	0.34	0.19	0.45	0.31
FT (Kim et al., 2018)	66.62	66.56	69.04	67.43	68.63	70.14
FT + AUKT	66.73	67.12	69.66	67.60	69.13	71.33
Δ	0.11	0.27	0.62	0.17	0.50	1.19

Baselines. We evaluate the Top-1 accuracy of multiple baseline methods, comparing their performance with and without the integration of **AUKT**. The baselines include KD (Hinton, 2015), FitNet (Romero et al., 2014), PKT (Passalis & Tefas, 2018), and FT (Kim et al., 2018).

Experimental Results. We first analyze the results of the homogeneous teacher-student framework under domain shift Level 1. As observed in Table 1, the Top-1 accuracy of all knowledge transfer methods improves when combined with **AUKT**, demonstrating the effectiveness of **AUKT** in enhancing model performance compared to conventional knowledge transfer techniques. Notably, in the ResNet56-ResNet20 case, the pretrained teacher performs worse than a student trained from scratch, leading to suboptimal performance after knowledge transfer. This highlights a key limitation of traditional knowledge transfer methods, which fail to account for teacher uncertainty, potentially resulting in degraded student performance. However, when combined

with **AUKT**, all methods achieve better results, with FitNet (Romero et al., 2014) even surpassing the performance of a student trained from scratch.

To further validate **AUKT**, particularly in scenarios where the teacher model underperforms, we evaluate it under a more significant domain shift, Level 2. Traditional knowledge transfer methods typically assume that the teacher model is both reliable and superior to the student. However, as shown in Table 2, when the teacher performs worse than the student under a larger domain shift, these methods often lead to degraded performance, resulting in students that perform worse than those trained from scratch. In contrast, integrating **AUKT** not only improves model performance but also enables the student to surpass the performance of a student trained from scratch. These findings highlight **AUKT**'s effectiveness in enhancing knowledge transfer, even when the teacher is unreliable, and demonstrate its superior adaptability to domain shifts. By selectively lever-

aging useful knowledge while avoiding misleading supervision, **AUKT** ensures robust student learning, allowing for better transferability of knowledge in challenging scenarios.

Finally, as part of our ablation studies, we evaluate the performance of a heterogeneous teacher-student framework and present the results in Table 4 in the Appendix. The table shows that, for all knowledge transfer methods, performance improves when combined with **AUKT**, further validating the effectiveness of our approach across different teacher-student structures.

4.2. Imitation-Guided Reinforcement Learning

For imitation-guided reinforcement learning, we demonstrate how **AUKT** improves policy learning efficiency and knowledge transferability in challenging and unseen environments when domain shifts occur compared to conventional knowledge transfer methods.

Experimental Settings. We evaluate **AUKT** across three gridworld environment scenarios, as illustrated in Fig. 4. For the environment details, please refer to the Appendix A.4.1. We collect expert demonstration data for the Lava 1 and Door environments to train imitation learning (IL) models via behavior cloning. The Lava 2 environment represents a domain-shifted variant of Lava 1, featuring modified environmental configurations. Importantly, we do not collect expert demonstration data for Lava 2, and no IL model is trained on this environment. This setup highlights the evaluation of our framework’s ability to generalize effectively under domain shifts, testing its generalization in unseen scenarios. After training the imitation learning (IL) models, we utilize them as teacher models, f_T , to guide the reinforcement learning (RL) agent during training, referred to as the student model, f_S . In this setup, we use the size of the prediction set to directly quantify model uncertainty—larger prediction sets correspond to higher uncertainty (Vovk et al., 2016). We use an error rate $\alpha = 0.1$ to construct the prediction set.

For a given state s , the guidance weight, as described in Section 3.3.2, is defined as: $w(s) = 1$ when $u_T(s) < u_S(s)$, otherwise $w(s) = 0$. Based on $w(s)$, we dynamically decide which action to take: $a = a_T$ if $w(s) = 1$, otherwise $a = a_S$. To encourage exploration by the RL agent, we define a probability $\epsilon = \min(0.5 \frac{t}{S_{total}} + 0.5 \frac{e}{E_{total}}, 1)$, where t is the current training step, e is the current episode, S_{total} and E_{total} are the total training steps and episodes, respectively. At each step, if a random probability $p < \epsilon$, the agent takes an action from the RL policy, otherwise it takes an action based on **AUKT**. As ϵ increases over time, the agent progressively shift to a learned RL policy, while initially it relies more on the IL model through **AUKT** to facilitate learning. Furthermore, we explore another soft variant of **AUKT**, instead of taking argmax to compare teacher and student prediction uncertainties, we define $w(s)$ as a probability dis-

tribution informed by the relative uncertainties of the teacher and student models: $w(s) = \frac{\exp(-u_T(s)/T)}{\exp(-u_T(s)/T) + \exp(-u_S(s)/T)}$, where T is the temperature to control the distribution sharpness with $T = 1$. And we sample the action a according to this distribution for $a \in \{a_T, a_S\}$.

Baselines. We compare **AUKT** and Soft **AUKT** against several baselines, including (1) SAC (Haarnoja et al., 2018), a purely RL approach, (2) IBRL (Hu et al., 2023), which leverages a pretrained imitation learning (IL) model to bootstrap RL. During the training process, IBRL queries the target Q-network and selects actions by comparing the Q-values of two candidate actions, a_T and a_S , and taking the action with the higher Q-value, and (3) Soft IBRL (Hu et al., 2023), a probabilistic variant of IBRL. Instead of selecting the action via a hard argmax, Soft IBRL samples the action according to a distribution proportional to the Q-values, $a \sim p(a) \propto \exp(\beta Q(s, a))$ for $a \in \{a_T, a_S\}$.

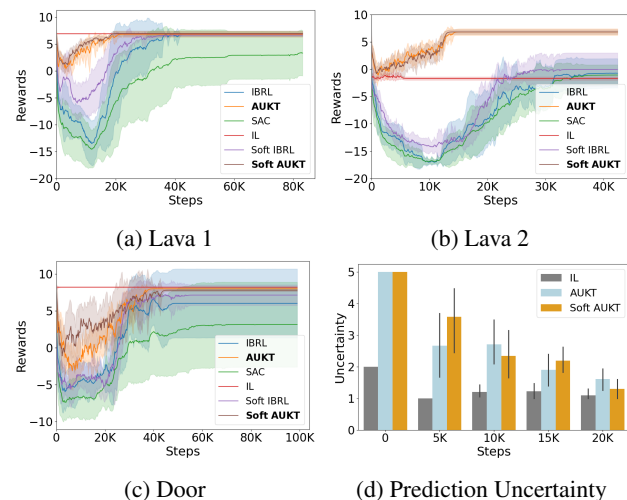


Figure 3. (a-c) Learning Curves. We compare **AUKT** and Soft **AUKT** with other baselines, including SAC, IBRL, and Soft IBRL, and present their learning curves across three environments: (a) Lava 1, (b) Lava 2, and (c) Door. **AUKT** and Soft **AUKT** perform similarly, converging faster and achieving higher rewards than other baselines in all environments. **(d) Prediction Uncertainty.** We show the average prediction uncertainties of **AUKT** and Soft **AUKT**, taking the Lava 1 environment as the example. Over time, their uncertainties shrink and approach that of the IL model, demonstrating the development of a well-learned RL policy.

Experimental Results. We present the experimental results in Fig. 3. First, we compare the learning curves of **AUKT** and Soft **AUKT** against other baselines across three environments: Lava 1, Lava 2, and Door. Both **AUKT** and Soft **AUKT** demonstrate similar performance, converging faster and achieving higher rewards than all other baselines. Before the agent reaches the goal, the reward function is defined as the negative Manhattan distance between the agent’s current location and the goal, normalized by the

maximum step limit of 100. Consequently, the accumulated episode rewards initially decrease as the agent explores the environment and accrues negative rewards but increase as it learns. The rewards of **AUKT** and Soft **AUKT** are consistently higher than those of other baselines and exhibit smaller initial decreases while converging faster. This can be attributed to the efficiency of **AUKT**, as it compares the prediction uncertainties of teacher and student models instead of relying on Q-values. Methods like IBRL and Soft IBRL, which depend on Q-values to decide between IL or RL actions, may make suboptimal decisions initially due to poorly trained Q-networks. For instance, even if an IL action is superior, its Q-value might be lower than that of an RL action.

In the domain-shifted environment Lava 2, the overall rewards of the IL model are lower due to the domain shift. IBRL and Soft IBRL rewards eventually converge close to the IL model’s performance, as these methods are not uncertainty-aware. Blindly relying on a teacher underperforming due to domain shifts can lead to suboptimal knowledge transfer. In contrast, **AUKT** and Soft **AUKT** consider the teacher’s prediction uncertainty, enabling significantly faster convergence and achieving rewards over six times higher than the best-performing baselines after convergence. When the teacher’s predictions are confident, the student relies more on them; otherwise, the student explores independently, enhancing knowledge transfer. Even though the teacher IL model’s overall reward is not high, it still provides useful knowledge. This allows the RL agent to learn from the teacher and eventually achieve higher rewards than the IL model. We also show the average model prediction uncertainties of **AUKT** and Soft **AUKT**, taking Lava 1 environment as the example, as illustrated in Fig. 3d. Over time, their uncertainties decrease and approach that of the IL model, demonstrating the progression toward a well-learned RL policy.

4.3. Autonomous Driving

In this section, we evaluate the performance of **AUKT** in the context of autonomous driving against other knowledge transfer baselines under domain shifts and noisy sensor inputs. The task involves learning a steer prediction policy using a multimodal teacher and an RGB-only student.

Experimental Settings. We adopt mean accuracy (mAcc) as the evaluation metric for the regression task of steer prediction, following prior works (Shen et al., 2021; 2023; 2024). We use the real-world driving dataset SullyChen (Chen, 2018) for evaluation, which includes diverse driving scenarios with various road types and conditions. We use Nvidia PilotNet (Bojarski, 2016) as the backbone for both the teacher and student models. The teacher model is a multimodal network that takes RGB images, depth and edge maps as input, while the student model is unimodal,

relying solely on RGB images. For more details of experimental settings, please see the Appendix A.5.1. We first train the teacher model f_T offline. Then we use it to guide the student model f_S training through knowledge transfer, while the RGB images for f_S training has domain shifts compared to the ones used for f_T training. Detailed information about domain shifts and model training can be found in Appendices A.5.2 and A.5.3, respectively.

Baselines. We use following knowledge transfer approaches as baselines, comparing their performance with and without the integration of **AUKT**. The baselines include KD (Hinton, 2015), FitNet (Romero et al., 2014), PKT (Passalis & Tefas, 2018), and FT (Kim et al., 2018).

Table 3. Mean accuracy (%) of steer prediction of different knowledge transfer methods with and without **AUKT** under domain shifts.

Approach	Mean Accuracy (%)		
	without AUKT	with AUKT	Δ
KD (Hinton, 2015)	73.5	76.8	3.3
FitNet (Romero et al., 2014)	72.4	76.2	3.8
PKT (Passalis & Tefas, 2018)	72.8	75.9	3.1
FT (Kim et al., 2018)	73.1	76.4	3.3
Teacher (RGB+Depth+Edge)	78.5		
Student (RGB)	71.8		

Experimental Results. We present the mean accuracy of steer prediction for various knowledge transfer methods with and without **AUKT** under domain shifts in Table 3. As observed, incorporating **AUKT** consistently enhances the accuracy of all knowledge transfer methods. This demonstrates the effectiveness of **AUKT** in improving model performance, as its adaptive guidance mechanism strategically balances the exploitation of teacher knowledge with the student’s own exploration. By preventing over-reliance on uncertain teacher predictions, **AUKT** facilitates more reliable and transferable knowledge under domain shifts.

5. Conclusions

We propose **AUKT**, a novel framework that leverages conformal prediction to efficiently quantify uncertainty in the teacher’s predictions for knowledge transfer. By dynamically adjusting the teacher’s influence based on confidence, **AUKT** ensures effective student learning, especially under domain shifts where traditional methods struggle due to over-reliance on uncalibrated teachers. Our approach selectively utilizes reliable guidance while avoiding misleading supervision and can still extract useful “dark knowledge” even when the teacher underperforms, unlike conventional methods that assume a superior teacher. **AUKT** is universal and domain-agnostic, making it applicable across diverse tasks. We validate **AUKT** on image classification, imitation-guided reinforcement learning, and autonomous driving, demonstrating improved performance, robustness, and transferability. For limitations and future work, please see the Appendix A.6.

Impact Statement

This paper presents work whose goal is to advance the field of machine learning, especially knowledge transfer with teacher-student structures. There are many potential societal consequences of our work, none of which we feel must be specifically highlighted here.

References

Abdar, M., Pourpanah, F., Hussain, S., Rezazadegan, D., Liu, L., Ghavamzadeh, M., Fieguth, P., Cao, X., Khosravi, A., Acharya, U. R., et al. A review of uncertainty quantification in deep learning: Techniques, applications and challenges. *Information fusion*, 76:243–297, 2021.

Angelopoulos, A., Bates, S., Malik, J., and Jordan, M. I. Uncertainty sets for image classifiers using conformal prediction. *arXiv preprint arXiv:2009.14193*, 2020.

Angelopoulos, A. N. and Bates, S. A gentle introduction to conformal prediction and distribution-free uncertainty quantification. *arXiv preprint arXiv:2107.07511*, 2021.

Bhaskar, A., Mohammad, Z., Jadhav, S. R., and Tokekar, P. Planrl: A motion planning and imitation learning framework to bootstrap reinforcement learning. *arXiv preprint arXiv:2408.04054*, 2024.

Bojarski, M. End to end learning for self-driving cars. *arXiv preprint arXiv:1604.07316*, 2016.

Chen, S. A collection of labeled car driving datasets. *Collection of labeled car driving datasets*, 2018.

Chevalier-Boisvert, M., Dai, B., Towers, M., Perez-Vicente, R., Willems, L., Lahlou, S., Pal, S., Castro, P. S., and Terry, J. Minigrid & miniworld: Modular & customizable reinforcement learning environments for goal-oriented tasks. *Advances in Neural Information Processing Systems*, 36, 2024.

Edupuganti, V., Mardani, M., Vasanawala, S., and Pauly, J. Uncertainty quantification in deep mri reconstruction. *IEEE Transactions on Medical Imaging*, 40(1):239–250, 2020.

Feng, Z., Guo, Y., and Sun, Y. Cekd: Cross-modal edge-privileged knowledge distillation for semantic scene understanding using only thermal images. *IEEE Robotics and Automation Letters*, 8(4):2205–2212, 2023.

Gao, P. and Zhang, H. Bayesian deep graph matching for correspondence identification in collaborative perception. In *Robotics Science and Systems (RSS)*, 2021.

Gao, P., Zhu, Q., and Zhang, H. Uncertainty-aware correspondence identification for collaborative perception. *Autonomous Robots*, 47(5):635–648, 2023.

Gu, Y., Dong, L., Wei, F., and Huang, M. Knowledge distillation of large language models. *arXiv preprint arXiv:2306.08543*, 2023.

Haarnoja, T., Zhou, A., Abbeel, P., and Levine, S. Soft actor-critic: Off-policy maximum entropy deep reinforcement learning with a stochastic actor. In *International conference on machine learning*, pp. 1861–1870. PMLR, 2018.

He, K., Zhang, X., Ren, S., and Sun, J. Deep residual learning for image recognition. In *Proceedings of the IEEE conference on computer vision and pattern recognition*, pp. 770–778, 2016.

Hinton, G. Distilling the knowledge in a neural network. *arXiv preprint arXiv:1503.02531*, 2015.

Hu, H., Mirchandani, S., and Sadigh, D. Imitation bootstrapped reinforcement learning. *arXiv preprint arXiv:2311.02198*, 2023.

Hu, J., Shen, L., and Sun, G. Squeeze-and-excitation networks. In *Proceedings of the IEEE conference on computer vision and pattern recognition*, pp. 7132–7141, 2018.

Huo, F., Xu, W., Guo, J., Wang, H., and Guo, S. C2kd: Bridging the modality gap for cross-modal knowledge distillation. In *Proceedings of the IEEE/CVF Conference on Computer Vision and Pattern Recognition*, pp. 16006–16015, 2024.

Jin, Y., Wang, J., and Lin, D. Multi-level logit distillation. In *Proceedings of the IEEE/CVF Conference on Computer Vision and Pattern Recognition*, pp. 24276–24285, 2023.

Karimi, H. and Samavi, R. Quantifying deep learning model uncertainty in conformal prediction. In *Proceedings of the AAAI Symposium Series*, volume 1, pp. 142–148, 2023.

Kim, J., Park, S., and Kwak, N. Paraphrasing complex network: Network compression via factor transfer. *Advances in neural information processing systems*, 31, 2018.

Kingma, D. P. Adam: A method for stochastic optimization. *arXiv preprint arXiv:1412.6980*, 2014.

Krizhevsky, A., Hinton, G., et al. Learning multiple layers of features from tiny images. 2009.

Kwon, Y., Won, J.-H., Kim, B. J., and Paik, M. C. Uncertainty quantification using bayesian neural networks in classification: Application to biomedical image segmentation. *Computational Statistics & Data Analysis*, 142: 106816, 2020.

Lu, C., Angelopoulos, A. N., and Pomerantz, S. Improving trustworthiness of ai disease severity rating in medical imaging with ordinal conformal prediction sets. In *International Conference on Medical Image Computing and Computer-Assisted Intervention*, pp. 545–554. Springer, 2022.

Ma, N., Zhang, X., Zheng, H.-T., and Sun, J. Shufflenet v2: Practical guidelines for efficient cnn architecture design. In *Proceedings of the European conference on computer vision (ECCV)*, pp. 116–131, 2018.

Michelmore, R., Wicker, M., Laurenti, L., Cardelli, L., Gal, Y., and Kwiatkowska, M. Uncertainty quantification with statistical guarantees in end-to-end autonomous driving control. In *2020 IEEE international conference on robotics and automation (ICRA)*, pp. 7344–7350. IEEE, 2020.

Mossina, L., Dalmau, J., and Andéol, L. Conformal semantic image segmentation: Post-hoc quantification of predictive uncertainty. In *Proceedings of the IEEE/CVF Conference on Computer Vision and Pattern Recognition*, pp. 3574–3584, 2024.

Passalis, N. and Tefas, A. Learning deep representations with probabilistic knowledge transfer. In *Proceedings of the European Conference on Computer Vision (ECCV)*, pp. 268–284, 2018.

Ranftl, R., Bochkovskiy, A., and Koltun, V. Vision transformers for dense prediction. In *Proceedings of the IEEE/CVF international conference on computer vision*, pp. 12179–12188, 2021.

Romero, A., Ballas, N., Kahou, S. E., Chassang, A., Gatta, C., and Bengio, Y. Fitnets: Hints for thin deep nets. *arXiv preprint arXiv:1412.6550*, 2014.

Saad-Falcon, J., Khattab, O., Santhanam, K., Florian, R., Franz, M., Roukos, S., Sil, A., Sultan, M. A., and Potts, C. Udapdr: unsupervised domain adaptation via llm prompting and distillation of rerankers. *arXiv preprint arXiv:2303.00807*, 2023.

Sandler, M., Howard, A., Zhu, M., Zhmoginov, A., and Chen, L.-C. Mobilenetv2: Inverted residuals and linear bottlenecks. In *Proceedings of the IEEE conference on computer vision and pattern recognition*, pp. 4510–4520, 2018.

Shafer, G. and Vovk, V. A tutorial on conformal prediction. *Journal of Machine Learning Research*, 9(3), 2008.

Shen, Y., Zheng, L., Shu, M., Li, W., Goldstein, T., and Lin, M. Gradient-free adversarial training against image corruption for learning-based steering. *Advances in Neural Information Processing Systems*, 34:26250–26263, 2021.

Shen, Y., Wang, X., Gao, P., and Lin, M. Auxiliary modality learning with generalized curriculum distillation. In *International Conference on Machine Learning*, pp. 31057–31076. PMLR, 2023.

Shen, Y., Zheng, L., Zhou, T., and Lin, C. Task-driven domain-agnostic learning with information bottleneck for autonomous steering. In *2024 IEEE International Conference on Robotics and Automation (ICRA)*, pp. 6858–6865. IEEE, 2024.

Simonyan, K. Very deep convolutional networks for large-scale image recognition. *arXiv preprint arXiv:1409.1556*, 2014.

Soria, X., Sappa, A., Humanante, P., and Akbarinia, A. Dense extreme inception network for edge detection. *Pattern Recognition*, 139:109461, 2023.

Sun, S., Ren, W., Li, J., Wang, R., and Cao, X. Logit standardization in knowledge distillation. In *Proceedings of the IEEE/CVF Conference on Computer Vision and Pattern Recognition*, pp. 15731–15740, 2024.

Sutskever, I., Martens, J., Dahl, G., and Hinton, G. On the importance of initialization and momentum in deep learning. In *International conference on machine learning*, pp. 1139–1147. PMLR, 2013.

Tian, Y., Krishnan, D., and Isola, P. Contrastive representation distillation. *arXiv preprint arXiv:1910.10699*, 2019.

Tibshirani, R. J., Foygel Barber, R., Candes, E., and Ramdas, A. Conformal prediction under covariate shift. *Advances in neural information processing systems*, 32, 2019.

Torabi, F., Warnell, G., and Stone, P. Behavioral cloning from observation. *arXiv preprint arXiv:1805.01954*, 2018.

Vovk, V., Fedorova, V., Nouretdinov, I., and Gammerman, A. Criteria of efficiency for conformal prediction. In *Conformal and Probabilistic Prediction with Applications: 5th International Symposium, COPA 2016, Madrid, Spain, April 20-22, 2016, Proceedings 5*, pp. 23–39. Springer, 2016.

Vovk, V., Petej, I., Toccaceli, P., Gammerman, A., Ahlberg, E., and Carlsson, L. Conformal calibrators. In *conformal and probabilistic prediction and applications*, pp. 84–99. PMLR, 2020.

Wang, S., Yan, Z., Zhang, D., Wei, H., Li, Z., and Li, R. Prototype knowledge distillation for medical segmentation with missing modality. In *ICASSP 2023-2023 IEEE International Conference on Acoustics, Speech and Signal Processing (ICASSP)*, pp. 1–5. IEEE, 2023.

Xue, Z., Gao, Z., Ren, S., and Zhao, H. The modality focusing hypothesis: Towards understanding crossmodal knowledge distillation. *arXiv preprint arXiv:2206.06487*, 2022.

Yang, Z., Pang, T., Feng, H., Wang, H., Chen, W., Zhu, M., and Liu, Q. Self-distillation bridges distribution gap in language model fine-tuning. *arXiv preprint arXiv:2402.13669*, 2024.

Yu, P., Mishra, M., Koppel, A., Busart, C., Narayan, P., Manocha, D., Bedi, A., and Tokek, P. Beyond joint demonstrations: Personalized expert guidance for efficient multi-agent reinforcement learning. *arXiv preprint arXiv:2403.08936*, 2024.

Zagoruyko, S. Wide residual networks. *arXiv preprint arXiv:1605.07146*, 2016.

Zagoruyko, S. and Komodakis, N. Paying more attention to attention: Improving the performance of convolutional neural networks via attention transfer. *arXiv preprint arXiv:1612.03928*, 2016.

Zhang, X., Zhou, X., Lin, M., and Sun, J. Shufflenet: An extremely efficient convolutional neural network for mobile devices. In *Proceedings of the IEEE conference on computer vision and pattern recognition*, pp. 6848–6856, 2018.

Zhao, R., Wang, K., Xiao, Y., Gao, F., and Gao, Z. Leveraging monte carlo dropout for uncertainty quantification in real-time object detection of autonomous vehicles. *IEEE Access*, 2024.

A. Appendix

A.1. Adaptive Uncertainty-Guided Knowledge Transfer (AUKT) Algorithm

Algorithm 1 Adaptive Uncertainty-Guided Knowledge Transfer (AUKT)

Require:

- 1: Pretrained teacher model f_T , student model f_S
- 2: Calibration set \mathcal{D}_{cal} from the student domain
- 3: Training set \mathcal{D}_{train}^S from the student domain

Ensure: Trained student model f_S

4: **Step 1: Calibrate Conformal Teacher Predictor**

- 5: Compute nonconformity scores $s_i = s(\bar{x}_i, \bar{y}_i)$ for each sample (\bar{x}_i, \bar{y}_i) from the calibration set \mathcal{D}_{cal}
- 6: Compute the $(1 - \alpha)$ -quantile $q_{1-\alpha}$ of the nonconformity scores

7: **Step 2: Train Student Model**

- 8: **for** each training sample $(x_j, y_j) \in \mathcal{D}_{train}^S$ **do**
- 9: Compute the teacher's prediction $f_T(x_j)$
- 10: Construct the conformal prediction set $\mathcal{C}(x_j)$ and compute $w(x_j)$ as in Eq. 3
- 11: Update the student model using the loss \mathcal{L} as in Eq. 2
- 12: **end for**

13: **return** Trained student model f_S

A.2. Theoretical Analysis

We provide a theoretical analysis comparing the proposed **AUKT** with standard knowledge transfer to explain why **AUKT** outperforms conventional methods, particularly under domain shifts. In **AUKT**, we leverage CP to quantify the teacher's prediction uncertainty and dynamically adjust its guidance to the student based on its prediction uncertainty. The adaptive uncertainty-guided loss function is follows:

$$\mathcal{L} = \lambda_1 \mathcal{L}_S + w(x) \cdot \lambda_2 \mathcal{L}_T, \quad (4)$$

where $\mathcal{L}_S(f_S(x), y)$ is the student's supervised task loss (e.g., mean square error, cross-entropy), $\mathcal{L}_T(f_S(x), f_T(x))$ is the teacher guidance loss (e.g., KL divergence, mean squared error), λ_1 and λ_2 are the coefficients, and w is an uncertainty-based weight derived from the teacher model's uncertainty u_T as in Eq. 3. The weight w approaches 1 when the teacher's predictions are confident and decreases toward 0 as the uncertainty increases, ensuring that the student relies more on the teacher's predictions when the uncertainty is low, and less when the uncertainty is high.

From the perspective of gradient modulation, taking the gradient of \mathcal{L} with respect to the student model parameter θ_S :

$$\nabla_{\theta_S} \mathcal{L} = \lambda_1 \nabla_{\theta_S} \mathcal{L}_S + w \lambda_2 \nabla_{\theta_S} \mathcal{L}_T, \quad (5)$$

when the teacher's prediction is confident, $w \rightarrow 1$, the gradient from teacher guidance loss is backpropagated to update the student model. Conversely, when the teacher's prediction is noisy, $w \rightarrow 0$, gradients from noisy \mathcal{L}_T are suppressed, preventing the student from learning incorrect patterns. However, standard knowledge transfer employs a fixed-weighted gradient update, $\nabla_{\theta_S} = \lambda_1 \nabla_{\theta_S} \mathcal{L}_S + \lambda_2 \nabla_{\theta_S} \mathcal{L}_T$, even if the teacher's prediction is noisy, the gradient from teacher guidance is backpropagated to update the student model, leading to suboptimal knowledge transfer.

Then we analyze from the perspective of critical point. To find the critical point of $f_S(x)$, we set the gradient of \mathcal{L} with respect to $f_S(x)$ to zero:

$$\frac{\partial \mathcal{L}}{\partial f_S(x)} = \lambda_1 \frac{\partial \mathcal{L}_S}{\partial f_S(x)} + w \lambda_2 \frac{\partial \mathcal{L}_T}{\partial f_S(x)} = 0. \quad (6)$$

Rearranging, the critical point $f_S^*(x)$ satisfies:

$$\frac{\partial \mathcal{L}_S}{\partial f_S(x)} = -\frac{w \lambda_2}{\lambda_1} \frac{\partial \mathcal{L}_T}{\partial f_S(x)}. \quad (7)$$

This equation implicitly defines $f_S^*(x)$ as a function of: the teacher's prediction $f_T(x)$, the ground truth label y , and the uncertainty-dependent weight w . When $w \rightarrow 1$ (low teacher prediction uncertainty), the student's prediction $f_S^*(x)$ aligns more closely with the teacher's prediction $f_T(x)$. When $w \rightarrow 0$ (high teacher prediction uncertainty), the student's prediction aligns more closely with the ground truth label y . However, in standard knowledge transfer,

$$\frac{\partial \mathcal{L}_S}{\partial f_S(x)} = -\frac{\lambda_2}{\lambda_1} \frac{\partial \mathcal{L}_T}{\partial f_S(x)}, \quad (8)$$

where the student consistently follows the teacher's guidance, limiting its capability to explore and learn new knowledge independently. When the teacher's prediction is noisy or there are domain shifts, this rigid reliance can lead to suboptimal knowledge transfer. While **AUKT** can adaptively adjust the teacher's guidance based on its prediction uncertainty, which effectively balances teacher knowledge exploitation and student exploration. This adaptive mechanism enhances the student's ability to generalize and improves the transferability of knowledge, particularly in domain-shifted environments.

Let's consider an example where \mathcal{L}_S and \mathcal{L}_T are mean square error (MSE) loss: $\mathcal{L}_S = \mathbb{E}_{(x,y)}[(f_S(x) - y)^2]$, $\mathcal{L}_T = \mathbb{E}_{(x,y)}[(f_S(x) - f_T(x))^2]$. The gradients:

$$\frac{\partial \mathcal{L}_S}{\partial f_S(x)} = 2(f_S(x) - y), \quad (9)$$

$$\frac{\partial \mathcal{L}_T}{\partial f_S(x)} = 2(f_S(x) - f_T(x)). \quad (10)$$

The critical point condition:

$$\lambda_1(f_S(x) - y) = -w\lambda_2(f_S(x) - f_T(x)). \quad (11)$$

Solving for $f_S(x)$:

$$f_S(x) = \frac{\lambda_1 y + w\lambda_2 f_T(x)}{\lambda_1 + w\lambda_2}. \quad (12)$$

As we can see from this equation, when $w \rightarrow 0$ (high teacher prediction uncertainty), $f_S(x) \rightarrow y$, the student model learns directly from the data and aims to approximate the ground truth y . Conversely, when $w \rightarrow 1$ (low teacher prediction uncertainty), $f_S(x) \rightarrow \frac{\lambda_1 y + \lambda_2 f_T(x)}{\lambda_1 + \lambda_2}$, which is a interpolation between teacher prediction $f_T(x)$ and ground truth y . However, standard knowledge transfer enforces strict adherence to the teacher's guidance, regardless of its accuracy, which can lead to suboptimal knowledge transfer, particularly when the teacher's predictions are noisy or domain shifts occur.

A.3. Image Classification

A.3.1. DIFFERENT LEVELS OF DOMAIN SHIFTS

We introduce two levels of domain shifts. In Level 1, we add Gaussian noise with zero mean and a standard deviation of 0.03 to 30% of the training data of 50K images, where the noisy samples are selected uniformly at random across the entire dataset to ensure consistent noise distribution. Then we shuffle the dataset and randomly split it into a 90% student training set \mathcal{D}_{train}^S , and a 10% calibration set \mathcal{D}_{cal} , ensuring that both sets are drawn from the same underlying distribution. Additionally, the same Gaussian noise is added to 30% of the testing data of 10K images, to form the noisy test set \mathcal{D}_{test} , which allows us to evaluate the performance of the models under noise conditions. In Level 2, the noise is increased to a zero mean with a standard deviation of 0.05, and we add it to 40% of the training and testing images. After introducing the noise, we again randomly split the training data into a 90% student training set \mathcal{D}_{train}^S , and a 10% calibration set \mathcal{D}_{cal} .

A.3.2. HETEROGENEOUS TEACHER-STUDENT STRUCTURE RESULTS

As part of our ablation studies, we evaluate the performance of a heterogeneous teacher-student framework and present the results in the following Table 4. The table shows that, for all knowledge transfer methods, performance improves when combined with **AUKT**, further validating the effectiveness of our approach across different teacher-student structures.

A.3.3. TRAINING DETAILS

For the experiments, we use the stochastic gradient descents (SGD) (Sutskever et al., 2013) as the optimizer with momentum 0.9 and weight decay $5e - 4$. The epoch number is 240 and the batch size is 64. The initial learning rate is set to 0.01 for MobileNet (Sandler et al., 2018)/ShuffleNet (Zhang et al., 2018) architectures and 0.05 for other architectures. The model is trained on an Nvidia RTX 3090 GPU with AMD Ryzen 9 5900 CPU and 32 GB RAM.

Table 4. Top-1 accuracy (%) of various knowledge transfer methods with and without **AUKT** on CIFAR-100 under heterogeneous structure and domain shift Level 1. We use Δ to show performance gain relative to conventional knowledge transfer methods without **AUKT**. We highlight in orange deltas greater than 0.15, indicating non-trivial enhancement following the protocol in (Sun et al., 2024).

	ResNet50	ResNet32 \times 4	VGG13	WRN-40-2
Teacher	72.99	73.01	70.65	69.38
Student	ShuffleNet-V1	MobileNet-V2	MobileNet-V2	ShuffleNet-V2
	65.66	57.22	57.22	66.91
KD (Hinton, 2015)	68.47	60.27	60.98	70.52
KD + AUKT	68.96	60.94	62.04	70.70
Δ	0.49	0.67	1.06	0.18
FitNet (Romero et al., 2014)	65.41	56.87	55.50	68.01
FitNet + AUKT	66.17	57.83	56.39	68.22
Δ	0.76	0.96	0.89	0.21
PKT (Passalis & Tefas, 2018)	65.16	57.33	56.22	67.20
PKT + AUKT	65.31	57.79	57.07	67.23
Δ	0.15	0.46	0.75	0.03
FT (Kim et al., 2018)	65.60	57.89	56.74	67.03
FT + AUKT	66.04	58.26	58.00	67.52
Δ	0.44	0.37	1.26	0.49

A.4. Imitation-Guided Reinforcement Learning

The environment scenarios shown in Fig. 4 are adapted from (Yu et al., 2024) and developed using the Minigrid framework (Chevalier-Boisvert et al., 2024). They are fully observable with discrete state and action spaces. In each environment, the agent's state corresponds to its $\{x, y\}$ coordinates on the map, and the action space comprises five discrete actions: *left*, *right*, *up*, *down*, and *stay*. Each episode is capped at a maximum of 100 steps. In the Lava 1 and Lava 2 environments, the reward function is computed as the negative Manhattan distance between the agent's current position and the goal, normalized by the maximum step limit of 100. Upon reaching the goal, the agent receives a terminal reward of $10 - 9 \times \frac{\text{step count}}{\text{max step}}$. Stepping into the lava results in a reward of -1, and the episode terminates immediately. Similarly, in the Door environment, the reward structure follows the same formulation but without lava, encouraging the agent to minimize its distance to the goal, with a same terminal reward applied upon successful completion.

We collect expert demonstration data comprising state-action pairs for the Lava 1 and Door environments to train imitation learning (IL) models via behavior cloning (Torabi et al., 2018). The demonstration data are inherently uncertain, as multiple valid actions may exist for the same state, as illustrated in (Yu et al., 2024), introducing ambiguity in the IL model's predictions.

A.4.1. ENVIRONMENT DETAILS

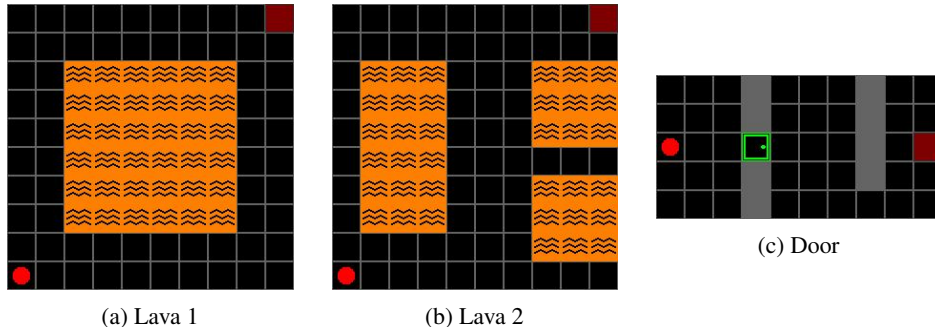


Figure 4. Gridworld Environment Scenarios. (a) **Lava 1**: An autonomous agent (red dot) must navigate to a target position (diagonal square) while avoiding lava regions. (b) **Lava 2**: A domain-shifted variant of Lava 1 with altered environment dynamics and layout. (c) **Door**: The agent must traverse a structured environment with doors and walls to reach the designated target position.

A.4.2. TRAINING DETAILS

For the imitation-guided reinforcement learning experiments, we employ a batch size of 512 and the Adam optimizer (Kingma, 2014) with an initial learning rate of $3e-4$. For each method and environment scenario, we train for 1000 episodes across 10 different random seeds. The model is trained on an Nvidia RTX 3090 GPU with AMD Ryzen 9 5900 CPU and 32 GB RAM.

A.5. Autonomous Driving

A.5.1. EXPERIMENTAL SETTINGS

We first define the accuracy with respect to a specific degree threshold τ as $acc_\tau = \text{count}(|\theta - \hat{\theta}| < \tau)/n$, following prior works (Shen et al., 2021; 2023; 2024), where n is the number of test cases; θ and $\hat{\theta}$ represent the ground truth and the predicted steer angle, respectively, for $\tau \in \mathcal{T} = \{1.5, 3.0, 7.5, 15.0\}$. Then we compute the mean accuracy (mAcc) by averaging acc_τ across different thresholds.

The SullyChen (Chen, 2018) dataset contains approximately 63,000 images, each with a resolution of 455×256 , paired with a corresponding steer angle annotation. We show some sample images in Fig. 5. To generate edge maps from RGB images, we employ DexiNed (Soria et al., 2023). To generate depth maps, we utilize DPT (Ranftl et al., 2021). Following (Shen et al., 2023), we use channel-level attention to represent the importance of each modality. For the teacher model f_T , we combine the data from different modalities (RGB, depth, and edge) at the channel level and pass them through an Squeeze-and-Excitation (SE) block (Hu et al., 2018), followed by a 1×1 convolution layer to make the channel number to be the same as the main modality RGB. We first train the teacher model f_T offline. Then we use it to guide the student model f_S training through knowledge transfer, while the RGB images for f_S training has domain shifts compared to the ones used for f_T training. For the details of domain shift, please refer to the Appendix A.5.2.

We use an error rate $\alpha = 0.1$ and compute nonconformity score s as the residuals between the predicted and true steer angles from the calibration set to get the quantile value $q_{1-\alpha}$. Then we use it to construct the prediction interval $\mathcal{C}(x)$ for a given input RGB image x . We define the teacher's uncertainty as the length of the prediction interval: $u_T(x) = |\mathcal{C}(x)|$. The dynamic weight is assigned as $w(x) = 1$ if $u_T(x) < \tau$, otherwise $w(x) = 0$, for $\tau \in \mathcal{T}$. For all knowledge transfer methods, we set the coefficients λ_1 and λ_2 in Eq. 2 to 1, assigning equal importance to the student task loss \mathcal{L}_S and the teacher guidance loss \mathcal{L}_T . Here, \mathcal{L}_S represents the MSE loss, while \mathcal{L}_T varies based on each knowledge transfer method.

A.5.2. DATA PROCESSING

After generating depth and edge maps, we split the dataset into 80% training and 20% testing. Then we train the multimodal teacher model on the training data offline. After training the teacher model, we introduce domain shift to the student training data compared to the teacher's pretraining data. Specifically, we add Gaussian noise with zero mean and a standard deviation of 0.1 to 30% of the RGB images of the training data, where the noisy samples are selected uniformly at random across the entire training set to ensure consistent noise distribution. We do not add Gaussian noise to the generated depth and edge maps, as they are not used for the student model. Then we shuffle the training data and randomly split it into a 90% student training set \mathcal{D}_{train}^S , and a 10% calibration set \mathcal{D}_{cal} , ensuring that both sets are drawn from the same underlying distribution. Additionally, the same Gaussian noise is added to 30% of the testing data of RGB images, to form the noisy test set \mathcal{D}_{test} , which allows us to evaluate the performance of the models under noise conditions.

A.5.3. TRAINING DETAILS

For the experiments, we employ a batch size of 32 and the Adam optimizer (Kingma, 2014) with an initial learning rate of $1e-3$, and a weight decay of $1e-5$. The model is trained on an Nvidia RTX 3090 GPU with AMD Ryzen 9 5900 CPU and 32 GB RAM for 240 epochs.

A.6. Limitations and Future Work

Despite the advantages of **AUKT**, there are some limitations. Currently, in our framework, the teacher model is pretrained and fixed during the knowledge transfer process, guiding the student without updates. Future work can explore more adaptive strategies where the teacher model is updated alongside the student, considering its prediction uncertainty. Such an extension could make the framework more flexible and better suited to handling domain shifts. Moreover, extending



Figure 5. Sample images of the real-world SullyChen dataset. SullyChen (Chen, 2018) is a real-world driving dataset which includes diverse driving scenarios with various road types and conditions.

AUKT to multi-teacher settings, where multiple sources of knowledge with varying expertise guide the student, presents an promising opportunity to further improve robustness and transferability, especially in complex, real-world applications.